Electrochemistry Communications 109 (2019) 106582

Contents lists available at ScienceDirect

Electrochemistry Communications

journal homepage: www.elsevier.com/locate/elecom

Acoustic emission as a function of polarisation: Diagnosis of polymer electrolyte fuel cell hydration state

V.S. Bethapudi[a,b], M. Maier[b], G. Hinds[c], P.R. Shearing[b], D.J.L. Brett[b,*], M.-O. Coppens[a,*]

[a] EPSRC "Frontier Engineering" Centre for Nature Inspired Engineering & Department of Chemical Engineering, University College London, London WC1E 7JE, United Kingdom

[b] Electrochemical Innovation Lab, Department of Chemical Engineering, University College London, London WC1E 7JE, United Kingdom

[c] National Physical Laboratory, Hampton Road, Teddington, Middlesex TW11 0LW, United Kingdom

ARTICLE INFO

Keywords:
Acoustic emission
Flushing
Start-up
In-operando
Flooding
Water management

ABSTRACT

Understanding water management is a crucial aspect in the development of improved polymer electrolyte fuel cells (PEFCs). Separating the performance degradation due to dehydration, water flooding and reactant starvation in PEFCs is a major challenge. In this study, acoustic emission (AE) analysis, a non-invasive and non-destructive diagnostic tool, is utilised to probe water formation and removal inside an operating fuel cell. In the acoustic emission as a function of polarisation (AEfP) method, AE activity from the PEFC is measured in terms of cumulative absolute AE energy (CAEE) hits during operation at discrete points on the polarisation curve. AEfP can identify the presence of liquid water in flow channels and correlate its formation and removal with the level of cell polarisation, and consequent internal temperature. Correlation between acoustic activity and water generation, supply and removal is achieved by varying current (polarisation), cathode air feed relative humidity (RH) and cell temperature, respectively. Features such as initial membrane hydration, liquid water formation, 'flushing' and the transition from 'wet-channel' to 'dry-channel' operation are identified using AE analysis, thereby providing a powerful and easy to implement diagnostic for PEFCs.

1. Introduction

Acoustic methods are emerging as powerful probes of the internal workings of electrochemical power systems and have the advantage of relatively low cost and non-invasive operation. These can be split into active measurements, where the relationship between a stimulus and the emerging sound wave are correlated to generate an image of the internal structure (e.g. ultrasound), and passive measurements [1], where probes 'listen' for events generated within the device (e.g. acoustic emission – AE).

Maier et al. used AE as a tool in characterising the flow conditions inside a polymer electrolyte membrane water electrolyser (PEMWE) [2]. The study observed correlations between the flow rates, current density and the corresponding acoustic parameters measured. Malzbender and Steinbrech measured the AE activity to characterise the thermo-mechanical aspects of solid oxide fuel cells [3]. As liquid water is produced and transported around a PEFC, it may be possible to identify its formation by measuring the generation of AE. To our knowledge, Legros et al. [4,5] were the first to utilise AE analysis as a water diagnostic tool for PEFC. Their initial reports indicated AE activity resulting from dehydration of the Nafion membrane and attributed it to structural changes occurring in the membrane during drying. A relationship between the ionic conductivity of the membrane and the AE activity of the PEFC was observed. Furthermore, AE from a PEFC was measured under different conditions, including without membrane electrode assembly (MEA), with MEA at open circuit voltage (OCV) and with MEA under load, respectively. These identified that hydrodynamics in the gas flow channels, water uptake and release by the MEA and electrochemical reactions can all contribute to the AE signal [5]. However, the benefits of the analysis are yet to be fully realised and greater understanding of how it can be applied to a PEFC under different operating conditions is required.

In this study, characterisation of a single-serpentine PEFC was performed under different operating conditions using AE measurements. The AE activity as a function of polarisation was determined across a range of humidity, temperature and current density. The electrochemical response was correlated with the acoustic response to deliver new insights into the water dynamics in an operational PEFC and, importantly, provide a means of separating performance degradation due to dehydration from that of reactant starvation.

* Corresponding authors at: Department of Chemical Engineering, University College London, Torrington Place, London WC1E 7JE, United Kingdom.
E-mail addresses: d.brett@ucl.ac.uk (D.J.L. Brett), m.coppens@ucl.ac.uk (M.-O. Coppens).

https://doi.org/10.1016/j.elecom.2019.106582
Received 8 October 2019; Received in revised form 23 October 2019; Accepted 24 October 2019
Available online 31 October 2019

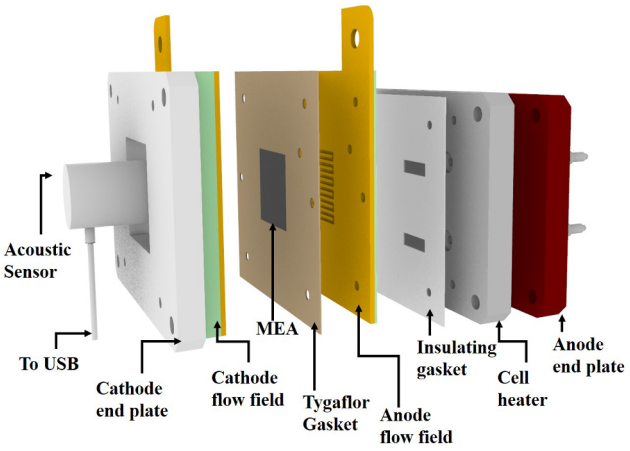

Fig. 1. Schematic diagram of PCB-based PEFC used in this work, with acoustic sensor (transducer) located on the cathode side of the fuel cell.

2. Experimental

2.1. PEFC design

The PEFC studied had 1 mm^2 square channel single-serpentine anode and cathode flow-fields developed on Au-coated printed circuit board (PCB) plates. PCB-based fuel cells have been extensively reported, the benefits of which are leading to commercialisation of the technology [6]. Although applied here to a PCB fuel cell, the AE technique is applicable to any fuel cell technology or method of construction.

The MEA active area for the PEFCs tested was 6.25 cm^2 with Nafion 212 (DuPont, USA) as membrane and Pt catalyst coated gas diffusion electrodes with a catalyst loading of 0.4 $mg_{Pt}cm^{-2}$ HyPlat (HyPlat, South Africa) as electrodes. The overall PEFC assembly is shown in Fig. 1.

2.2. Testing of PEFC

A Scribner 850e fuel cell test station was used for the experimental studies, with hydrogen and air flow were maintained at constant flow rate of 100 mL min^{-1} and 500 mL min^{-1}, respectively. Cell heater, as in Fig. 1, was used to set the PEFC temperature. Polarisation measurements were carried out between open circuit voltage (OCV) and 0.3 V at intervals of 0.05 V, and 30 s hold at each voltage point. Before any polarisation, cell conditioning was performed, where the PEFC was supplied with reactants for 2 min for the stabilisation of gas flow and humidity in the channels.

Electrochemical impedance spectroscopy (EIS) measurements were performed using a Gamry Reference 3000 and Gamry Reference 30 k Booster (Gamry Instruments) in galvanostatic mode. The frequency range for analysis was 100 kHz to 0.1 Hz, with 10 points per decade, and an AC modulation amplitude of 5% of the DC (direct current) input signal.

2.3. Acoustic emission testing

Acoustic activity from the PEFC was measured using a piezoelectric acoustic sensor (S9208; Mistras NDT, UK) secured to the surface of the cathode flow-field plate, as shown in Fig. 1. The acoustic signal was collected, processed and analysed using the AEWin software (Physical Acoustics Corporation, USA). The sensor had a resonant frequency of 500 kHz and an operating frequency range of 200 kHz to 1000 kHz. The single channel AE acquisition system had lower and upper analogue filters of 20 kHz and 1 MHz, respectively, and a fixed threshold value of 27 dB, considering the background noise during testing; a signal beyond this threshold was recorded as an AE hit.

Any material undergoing a mechanical perturbation releases energy that results in the generation of elastic waves, which produce sound (AE) at a frequency and intensity commensurate with the energy released [7]. Fig. 2 illustrates a typical AE hit, consisting of established features like: amplitude (dB), counts, duration (μs), rise time (μs) and energy (aJ) [8].

In this study, the acoustic activity from the PEFC is computed based on three parameters: amplitude (dB), which is the peak AE signal excursion obtained in a hit; energy (aJ), which is the area under an AE hit generated; and counts, which is the number of excursions exceeding the AE threshold.

3. Results and discussion

3.1. Acoustic emission as a function polarisation (AEfP)

Polarisation curves, Fig. 3(a) and (c), and the corresponding acoustic emission as a function of polarisation (*AEfP*) curves, Fig. 3(b) and (d), were measured at reactant relative humidity (RH) levels of 40% RH, 70% RH and 100% RH, and at cell temperatures of 45 °C and 60 °C.

Considering points on the polarisation curves of equal current density as having the same rate of water generated (from the electrochemical reaction), RH as a measure of the water introduced to the cell from reactant flow, and temperature as a driving force for water to be removed from the cell, it is possible to analyse the AE results based on different cell hydration conditions.

At 45 °C cell temperature, a reduced cell performance was observed

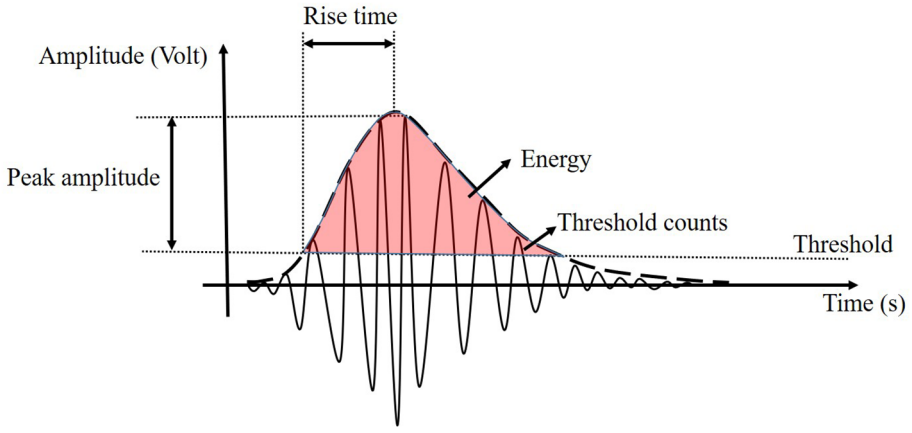

Fig. 2. Parametric representation of a typical AE hit, showing key parameters measured during a single event (adapted from [8]).

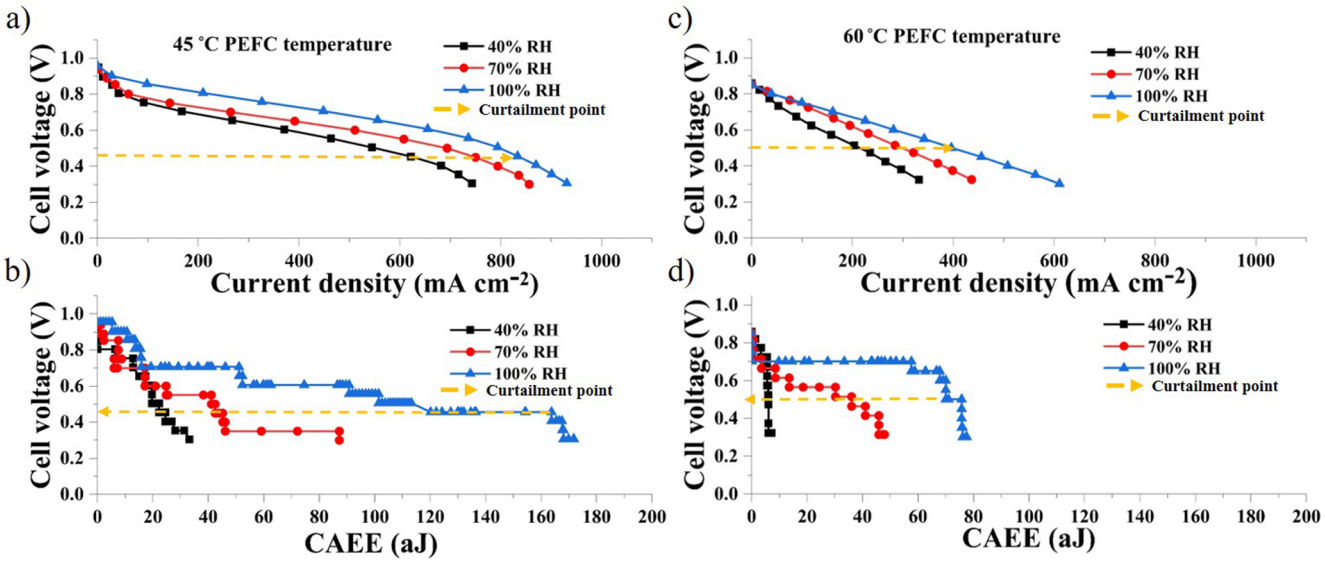

Fig. 3. (a) Polarisation curve of PEFC at 40%, 70% and 100% reactant RH – 45 °C cell temperature, (b) AEfP curve showing CAEE during polarisation – 45 °C cell temperature, (c) Polarisation curve of PEFC at 40%, 70% and 100% reactant RH – 60 °C cell temperature and (d) AEfP curve showing CAEE during polarisation – 60 °C cell temperature.

at 40% RH (Fig. 3(a)), which can be attributed to the decreased membrane conductivity arising from insufficient hydration [9]. Increasing the reactant humidity to 70% RH, and then 100% RH, resulted in continually improved cell performance, predominantly observed in the Ohmic region and attributed to the improved membrane hydration [10].

Over the conventional activation region of the polarisation curve (low current density), the cumulative absolute AE energy (CAEE) for each RH was similar. However, at higher current densities, increased RH led to increased AE activity. At 40% RH the CAEE increase was gradual and steady over the entire current density range, whereas at the higher RH levels a significant increase in CAEE was observed in the Ohmic region, with the 100% case, which attained the highest current density, showing curtailment of AE activity above ~850 mA cm^{-2}.

Such incremental development in CAEE with current density is primarily attributed to increased water generation from the electrochemical reaction (reactant's RH and velocity remained constant throughout the test in each case). It is well known, from the likes of neutron imaging studies [11,12], that, as current density increases, water initially builds up within the gas diffusion layer (GDL), primarily under the land regions, and then inhabits the flow channel itself. Release of liquid water into the channels, and particularly its impingement on channel walls at corners and switchbacks, is a source of AE. Higher RH tends to promote liquid water accumulation in the channels, which is consistent with the increasing CAEE observed in the Ohmic region with increasing RH (Fig. 3(b)).

Although the cell was externally heated to 45 °C, the local temperature of the cathode will increase based on reaction conditions. As current density increases, cell heating occurs and acts to drive off water, removing liquid water from channels and the GDL and potentially dehydrating the membrane [13,14]. The curtailment of CAEE (~0.45 V) and the corresponding current density of ~850 mA cm^{-2} at ~0.45 V for the 100% RH condition is consistent with removal of liquid water from channels due to the dehydrating action of a higher cell temperature (current).

At a higher externally set temperature, 60 °C, the cell will be more prone to dehydration. The cell performance (Fig. 3(c)) and acoustic polarisation (CAEE) (Fig. 3(d)) of the PEFC at all operating conditions decreased substantially (compared to 45 °C). At 40% RH, a very low level of CAEE was measured as a result of the higher set temperature that dehydrated the cell considerably. This excessive dehydration reduced membrane conductivity to a greater extent, such that the limiting current density delivered by the PEFC dropped to 350 mA cm^{-2} at 60 °C (from 743 mA cm^{-2} at 45 °C). Increasing the reactant RH to 70%, the cell performance improved, with an increase in CAEE observed over the entire polarisation range.

At 60 °C, the curtailment of CAEE is clearly observed for the 100% RH case during the transition from a 'wet channel' to 'dry channel' condition above ~400 mA cm^{-2}, as the local cathode temperature increases with current density. This transition is also evident for the 70% RH case from ~300 mA cm^{-2}.

To express the relative changes in membrane hydration under different conditions, measurements of high frequency resistance (HFR), as given in Fig. 4(a) and (b), and EIS, as given in Fig. 4(c), were carried out [15].

At 45 °C, there is a systematic difference in membrane resistance over the current range, with greater RH leading to lower membrane resistance, as expected. With increasing current density, there is a decrease in membrane resistance, as the membrane becomes increasingly hydrated due to the generation of product water. However, for the poorly humidified 40% RH condition, the increase in cell temperature associated with higher current density leads to membrane dehydration. This results in a steep increase in resistance beyond 600 mA cm^{-2}. At this cell temperature, the 70% and 100% RH flow conditions are sufficient to adequately hydrate the membrane. However, with an increase in set cell temperature to 60 °C, there is a rise in the HFR under all conditions, indicating a significant drop in membrane hydration. In addition, a significant increase in charge transport resistance (R_{ct}) is observed, as shown in Fig. 4(c) (EIS performed at 400 mA cm^{-2} current density). The corresponding R_{ct} measured indicated almost a 50% higher value at 60 °C compared to that measured at 45 °C, as presented in Table 1, indicating considerable membrane dehydration [16].

Overall, membrane resistance rapidly increases with current density (and local temperature) and limits the ability of the cell to deliver higher currents. These results, from the membrane hydration perspective, are consistent with reduction in the liquid water volume, derived from acoustic measurements, and collectively describe the cell hydration over the polarisation range.

3.2. Cell start-up and current hold

A galvanostatic test was performed on the PEFC at a current density

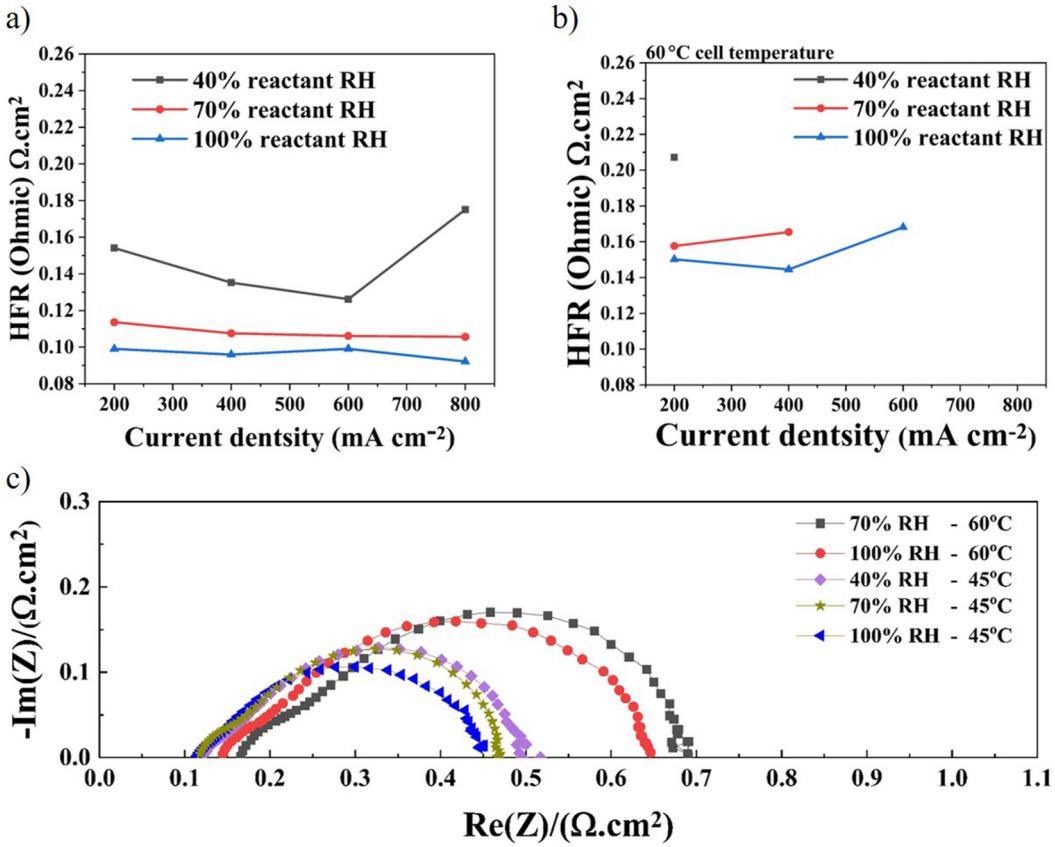

Fig. 4. High frequency resistance, HFR (an average of 3 measurements and reproducible within 0.006 Ω.cm^2) of the PEFC tested at 40%, 70% and 100% RH at (a) 45 °C cell temperature and (b) 60 °C cell temperature, and (c) EIS measurements at 400 mA cm^{-2} at 45 °C and 60 °C cell temperatures.

Table 1
Charge transfer (R_{ct}) resistances determined for PEFC at 45 °C and 60 °C cell temperature and 400 mA cm^{-2} current density.

Reactants RH	45 °C cell set temperature			60 °C cell set temperature	
	40%	70%	100%	70%	100%
R_{ct} (Ω.cm^2)	0.39	0.35	0.34	0.53	0.5

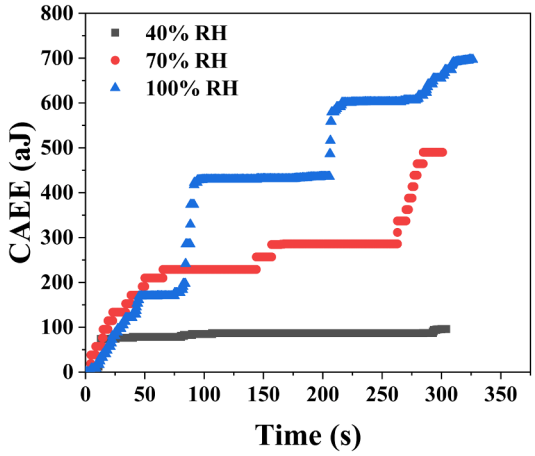

Fig. 5. CAEE response during galvanostatic test at 600 mA cm^{-2}, at 45 °C.

of 600 mA cm^{-2} and a cell temperature of 45 °C to examine initial start-up of the cell and dynamic performance over time. The corresponding CAEE is given in Fig. 5. Over the initial 0–25 s, the rate of CAEE increase for each of the RH conditions is similar and can be attributed to an equilibration phase, where flow, temperature and humidification factors stabilise, and the membrane hydrates (expands), as reported by Legros et al. [5].

Following the initial stabilisation period, the CAEE for the 40% RH case reaches a plateau, indicating dry-channel operation. On the other hand, the profiles for 70% and 100% RH exhibit an extended initial stabilisation phase of ~50 s, corresponding to more extensive hydration of the gases compared to the 40% RH case. Then follows periods of relative inactivity (plateaus), which can last upwards of 100 s, with relatively short intermittent periods of significant acoustic activity. This observation is consistent with the 'flushing' events commonly seen in PEFC operation [17,18].

As observed by the likes of dimensional change and neutron imaging measurements [12,17], as well as those generally experienced in fuel cell testing, water is typically expelled from a fuel cell sporadically during 'flushing' events. As water builds in the channels of a fuel cell, it will typically initially exist as sessile droplets [11,14]. Periodically, droplets detach as they grow and eventually become entrained in the reactant gas flow. These droplets can then act to dislodge other droplets, resulting in an 'avalanche' effect with resulting emission of sudden spurts of water from the cell. Neutron imaging has also identified the 'snaking' effect of water that becomes dislodged and coalesces into a 'long train' water droplet that makes its way through a cell with a similar sudden ejection of water [11].

4. Conclusions

The performance diagnosis of a PEFC under different experimental conditions, utilising the AE analysis, identified a strong correlation between PEFC performance and simultaneous acoustic activity

generated. The measured AE activity was able to indicate the cumulative and discrete effects of reactant humidity and operating conditions on the performance of the PEFC. Membrane dehydration was identified for PEFC operation at 40% reactant RH by polarisation and electrochemical characterisations. Corroboratively, lower AE activity was measured during these operational conditions, indicating membrane dehydration under low reactant humidity conditions. However, under higher reactant humidity conditions the PEFC performance improved with a simultaneous increase in the AE activity measured, confirming the influence of PEFC operation on AE activity. Increasing the cell temperature by 15 °C exacerbated the membrane dehydration, which was reflected in a severe drop in cell performance and acoustic signal. Furthermore, the dependency of AE activity on PEFC operating performance was also confirmed by the high-frequency and charge transfer resistances determined from EIS.

Declaration of Competing Interest

The authors declare that they have no known competing financial interests or personal relationships that could have appeared to influence the work reported in this paper.

Acknowledgements

The authors would like to acknowledge funding from the EPSRC “Frontier Engineering” Award (EP/K038656/1), and other funds from the EPSRC for supporting fuel cell research in the “Electrochemical Innovation Lab (EIL)” (EP/R023581/1, EP/P009050/1, EP/L015749/1, EP/M014371/1, EP/M023508/1, EP/M009394/1). We also thank the Department of Chemical Engineering, University College London, and the National Measurement System of the UK Department of Business, Energy and Industrial Strategy for supporting this work.

The authors would like to acknowledge Dr. Quentin Meyer and Professor Daniel Steingart for their assistance in sourcing the equipment and supplying the interfacing code used to obtain the data.

References

[1] J.B. Robinson, M. Maier, G. Alster, T. Compton, D.J.L. Brett, P.R. Shearing, Phys. Chem. Chem. Phys. 21 (2019) 6354–6361.
[2] M. Maier, Q. Meyer, J. Majasan, C. Tan, I. Dedigama, J. Robinson, J. Dodwell, Y. Wu, L. Castanheira, G. Hinds, P.R. Shearing, D.J.L. Brett, J. Power Sources 424 (2019) 138–149.
[3] J. Malzbender, R.W. Steinbrech, J. Power Sources 173 (2007) 60–67.
[4] B. Legros, P.-X. Thivel, Y. Bultel, M. Boinet, R.P. Nogueira, Electrochem. Solid-State Lett. 12 (2009) B116–B118.
[5] B. Legros, P.X. Thivel, Y. Bultel, M. Boinet, R.P. Nogueira, J. Power Sources 195 (2010) 8124–8133.
[6] R. O’Hayre, D. Braithwaite, W. Hermann, S.J. Lee, T. Fabian, S.W. Cha, Y. Saito, F.B. Prinz, J. Power Sources 124 (2003) 459–472.
[7] F. Man, IEEE Trans. Commun. 21 (1973) 1027–1031.
[8] W. Caesarendra, B. Kosasih, A.K. Tieu, H. Zhu, C.A.S. Moodie, Q. Zhu, Mech. Syst. Signal Process. 72–73 (2016) 134–159.
[9] F.B. Weng, B.S. Jou, C.W. Li, A. Su, S.H. Chan, J. Power Sources 181 (2008) 251–258.
[10] Y. Song, H. Xu, Y. Wei, H.R. Kunz, L.J. Bonville, J.M. Fenton, J. Power Sources 154 (2006) 138–144.
[11] Y. Wu, J.I.S. Cho, T.P. Neville, Q. Meyer, R. Zeische, P. Boillat, M. Cochet, P.R. Shearing, D.J.L. Brett, J. Power Sources 399 (2018) 254–263.
[12] Y. Wu, J.I.S. Cho, X. Lu, L. Rasha, T.P. Neville, J. Millichamp, R. Ziesche, N. Kardjilov, H. Markötter, P. Shearing, D.J.L. Brett, J. Power Sources 412 (2019) 597–605.
[13] Q. Meyer, S. Ashton, P. Boillat, M. Cochet, E. Engebretsen, D.P. Finegan, X. Lu, J.J. Bailey, N. Mansor, R. Abdulaziz, O.O. Taiwo, R. Jervis, S. Torija, P. Benson, S. Foster, P. Adcock, P.R. Shearing, D.J.L. Brett, Electrochim. Acta 211 (2016) 478–487.
[14] Y. Wu, Q. Meyer, F. Liu, L. Rasha, J.I.S. Cho, T.P. Neville, J. Millichamp, R. Ziesche, N. Kardjilov, P. Boillat, H. Markötter, I. Manke, M. Cochet, P. Shearing, D.J.L. Brett, J. Power Sources 414 (2019) 272–277.
[15] O.A. Obeisun, Q. Meyer, J. Robinson, C.W. Gibbs, A.R. Kucernak, P.R. Shearing, D.J.L. Brett, Int. J. Hydrogen Energy 39 (2014) 18326–18336.
[16] S. Asghari, A. Mokmeli, M. Samavati, Int. J. Hydrogen Energy 35 (2010) 9283–9290.
[17] T.J. Mason, J. Millichamp, T.P. Neville, P.R. Shearing, S. Simons, D.J.L. Brett, J. Power Sources 242 (2013) 70–77.
[18] A. Iranzo, A. Salva, P. Boillat, J. Biesdorf, E. Tapia, F. Rosa, Int. J. Hydrogen Energy 42 (2017) 13839–13849.